EFFICIENCY ENHANCEMENT OF A HARMONIC LASING FREE ELECTRON LASER

E. Salehi, Department of Physics, Amirkabir University of Technology, Tehran, Iran
N.S. Mirian*, UVSOR Facility, Institute for Molecular Science, Okazaki, Japan and
School of Particle and Accelerator Physics, Institute for Research in Fundamental Sciences (IPM), Tehran, Iran
B. Maraghechi, Department of Physics, Amirkabir University of Technology, Tehran, Iran

Abstract

The harmonic lasing free-electron laser amplifier, in which two wigglers is employed in order for the fundamental resonance of the second wiggler to coincide with the third harmonic of the first wiggler to generate ultraviolet radiation, is studied. A set of coupled nonlinear first-order differential equations describing the nonlinear evolution of the system, for a long electron bunch, is solved numerically by CYRUS code. Thermal effects in the form of longitudinal velocity spread are also investigated. The second wiggler field decreases linearly and nonlinearly at the point where the radiation of the third harmonic saturates to enhance the efficiency. The optimum starting point and the slope of the tapering of the amplitude of the wiggler are found by a successive run of the code. It is found that tapering can increase the saturated power of the third harmonic considerably.

INTRODUCTION

High-gain free-electron laser(FEL) amplifiers hold great prospects as high power, coherent, and tunable radiation in the x-ray regions of the electromagnetic spectrum. Utilizing nonlinear harmonic generation when bunching the harmonics is driven by the fundamental frequency in the vicinity of saturation is a possible way for obtaining x-ray wavelengths [1–7].

Recently, McNeil et al. [8] proposed a harmonic lasing FEL amplifier in a one-dimensional limit that can be extended to higher harmonics by suppressing the interaction at the fundamental resonance while allowing the harmonics to evolve to saturation. To suppress the interaction at the fundamental resonance without affecting the third harmonic lasing, they proposed two different settings for the undulator are considered by changing the wiggler magnetic field while keepingthe wiggler period, λ_w , and the initial average electron beam energy, γ, constant.

The intrinsic efficiency of the FEL is low. By increasing the energy of the electron beam, the efficiency reduces further. Therefore, for the x-ray FEL, efficiency is very low.For this reason, much attention has been givenin the literature to schemes for the FEL efficiency enhancement [9–13].

The purpose of the present study is to use the concept of the linear and nonlinear tapering of the wiggler field to increase the efficiency of the harmonic lasing FEL. To this end, by decreasing the wiggler amplitude linearly or nonlinearly at the saturation point, the resonance condition of the FEL is restored, which will result in higher intensity UV radiation. The slippage of the radiation with respect to the long electron bunch is ignored. Equations describing harmonic lasing FEL are derived. This set of equations is solved numerically using CYRUS 1D code in one-dimension [14]. CYRUS, which was developed by N. S. Mirian et al to study nonlinear harmonic generation. This code like MEDUSA employs nonaveraged equations [15,16]. The third harmonic lasing is considered so that the operating wavelength is in the ultraviolet (UV) domain.

BASIC EQUATIONS

The numerical simulation of the harmonic lasing is conducted using the CYRUS 1D code that is written in standard FORTRAN 90. This code like MEDUSA [15, 16] employs nonaveraged equations. The formulation treats the planar wiggler model and the radiation field is represented as a superposition of Gaussian modes [17]. The vector potential of the radiation field, in plane-polarized form, is

$$\delta\mathbf{A}(\mathbf{z},t)=\sum_{l,n,h}[\delta A_h^{(1)}sin(\varphi_h)+\delta A_h^{(2)}cos(\varphi_h)]\hat{\mathbf{e}_x} \qquad (1)$$

where $\delta A_h^{(i)}$ with $i = 1, 2$ are the amplitudes that are assumed to vary slowly in z and t and $h = 1, 3, \ldots$ denotes the harmonic number, $\alpha_h = h(k_0 z - \omega t)$ is the phase of the hth harmonic of the angular frequency ω. Averaging Maxwell's equations over the time scale $2\pi/\omega$, the field equations take the form

$$\left(\frac{\partial}{\partial z}\right)\begin{pmatrix}\delta a_h^{(1)}\\ \delta a_h^{(2)}\end{pmatrix}=\frac{\omega_b^2}{2h\omega c}\begin{pmatrix}\langle\frac{u_x}{|u_z|}cos\alpha_h\rangle\\ \langle-\frac{u_x}{|u_z|}sin\alpha_h\rangle\end{pmatrix} \qquad (2)$$

where $\delta a_h^{(i)} = e\delta A_h^{(i)}/m_e c^2$ are the normalized amplitudes, $\omega_b^2 = 4\pi e^2 n_b/m_e c^2$ is the square of the beam plasma frequency. The averaging operator is defined as

$$\langle(\cdots)\rangle=\int_0^{2\pi}\frac{\sigma(\psi_0)}{2\pi}d\psi_0\int_0^{\infty}dpG_0(p_z)(\cdots) \qquad (3)$$

.

Here, $\sigma(\psi_0)$ is the phase distribution at entry time. Also, $G_0(p_z)$ is the initial momentum space distribution which is

* nsmrian@ims.ac.jp

ISBN 978-3-95450-134-2

chosen to have a spread in the longitudinal momentum, in the form of a Gaussian distribution function, without any spread in the transverse momentum. We chose the thermal distribution function as

$$G_0(p_z) = \sqrt{\frac{2}{\pi}}\frac{1}{\triangle p_z} exp\left(-\frac{2(p_z - p_0)^2}{\triangle p_z^2}\right) \quad (4)$$

where p_0 and $\triangle p_z$ are the initial bulk momentum and momentum spread, respectively. Electron trajectories are integrated using the Lorentz force equations in the magnetostatic and electromagnetic fields. It is important to emphasize that no average is performed over the Lorentz force equation.

$$\frac{d\boldsymbol{P}}{dt} = -e\delta\mathbf{E} - \frac{e}{c}\mathbf{v}\times(\delta\mathbf{B} + \mathbf{B}_w) \quad (5)$$

Here $\mathbf{B}_w$ is the planar wiggler magnetic field in one dimension that is written as

$$\mathbf{B}_w(z) = B_w(z)sin(k_w z)\hat{e_y}.$$

The details of the formulation is explained in Ref. [18].

In this paper, we consider a harmonic lasing FEL in which the wiggler consists of two halves with two different magnetic field strengths but the same wavelength λ_w. We reduce the wavelength of the fundamental harmonic of the first part by reducing the rms wiggler $a_n = \overline{\Omega}_n/\sqrt{2}$ (for planar wiggler). Suppose that in the first part the rms wiggler parameter is a_1 and the fundamental resonant wavelength is λ_1 with the harmonic resonant wavelength $\lambda_h = \lambda_1/h$, $h = 3, 5, 7, \ldots$. In the second part the rms wiggler parameter is a_n so that the new resonant fundamental wavelength is the nth harmonic of the first mode setting, $\lambda_1' = \lambda_n$.We assume that the beam energy and the undulator period are fixed. Therefore the retuned wiggler parameter a_n is obtained from the FEL resonance relation:

$$\frac{1 + a_1^2}{1 + a_n^2} = n. \quad (6)$$

Obviously, there are no real solutions fora_n if $a_c = \sqrt{n-1}$.

NUMERICAL SIMULATION

The complete set of coupled nonlinear differential equations is solved numerically using the fourth-order Rounge-Kutta method. For the particle averaging, the Gaussian quadrature technique in each of the degrees of freedom (ψ_0, p_{z0}) is used. In this work, an attempt was made to match the third harmonic resonance of the first part of the wiggler to the fundamental resonance of the second part in order to obtain UV radiation. The common parameters of the wigglers, radiation, and the electron beam which are used in this study are as follows: the electron beam has the relativistic factor of 300 with peak current of 200A and the initial radius of 0.15 mm. The wavelength of both parts of the wiggler is 2.8 cm. The peak value of the on-axis amplitude of the first part of the wiggler is 8.33 KG over the length

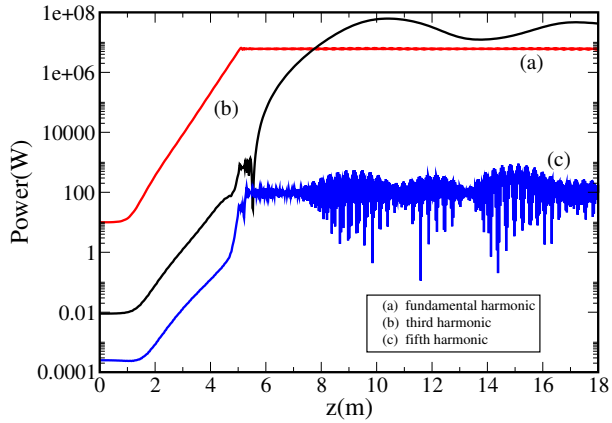

Figure 1: Power of the fundamental resonance (a), the third harmonic (b), and the fifth harmonic (c) versusz(m).

of 5 m, and the entry tapered region is $N_w = 10$ wiggler period in length. Using relation (6), we obtain $a_3 = 0.349$, and optimize the step taper and overall length for the maximum output. Using these beam and wiggler parameters, the fundamental resonance is at the wavelength of 523.9 nm, and the initial power is 10 W. The third harmonic resonance wavelength is 174.63 nm and starts from zero initial power. Figure 1 demonstrates the harmonic lasing scheme as described above. The resonant, cold beam limit is assumed. It is seen that the fundamental scaled intensity (a) is disrupted at $z = 5\,m$. Also, the intensity of the third harmonic (b), which is the fundamental of the second part of the wiggler when the undulator parameter is re-tuned at $\overline{\Omega}_3 = 0.49$, and the intensity of the fifth harmonic (c) are shown in Fig. 1. It is seen that the third harmonic grows to $3.8 \times 10^7 W$ and the fifth harmonic is also disrupted.

Figure 2 shows the longitudinal phase space of the electrons at different coordinates z along the wiggler for $\triangle\gamma/\gamma = 0.002$. Plots (a), (b), and (c) are for the first part of the wiggler and plots (d), (e), and (f) are related to the second part. The uneven distribution of initial phase, in plot (a), is the artifact of the Gauss quadrature weightings. Observe that as electrons move along the wiggler their energy gets redistributed in pondermotive phase $\psi = \alpha_3 + k_w z$ along a straight line with a sinusoidal modulation. This straight line is an indication of the energy spread. It is evident that the spread of energy becomes progressively larger as the beam approaches the saturation point. At $z = 6\,m$, the sinusoidal modulation is an indication that the untrapped electrons move along and pass over the pondermotive potential. The trapped particle at saturation is shown by the non-sinusoidal phase-space plot at $z = 17\,m$. We can conclude, therefore, that the plot of γ versus ψ truly represents the conventional phase space of $d\psi/dz$ versus ψ. Also, the variations of energy of the electrons is shown in Fig. 3 as a function of the distance through the wiggler. It is seen that the energy of the electrons after saturation point changes oscillationary.

The radiation intensity, $|A|$, indicates the efficiency of the FEL system. The lower (higher) intensity yields a lower

ISBN 978-3-95450-134-2

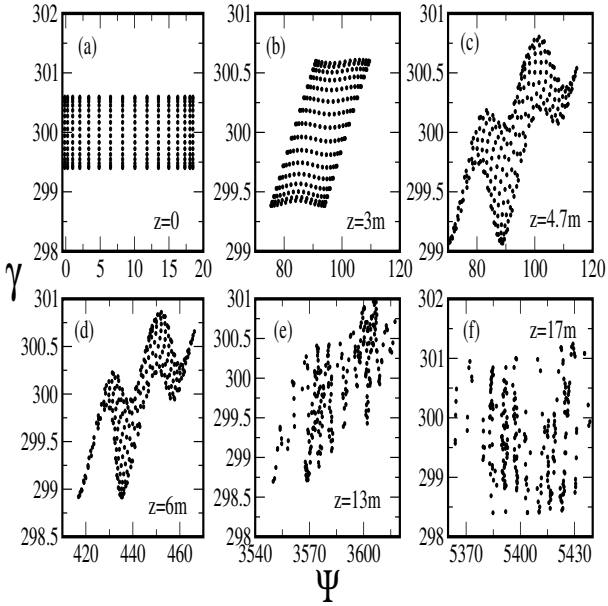

Figure 2: Distribution of energy γ versus the distribution of pondermotive phase of the electron beam at different values of the coordinate z along the undulator.

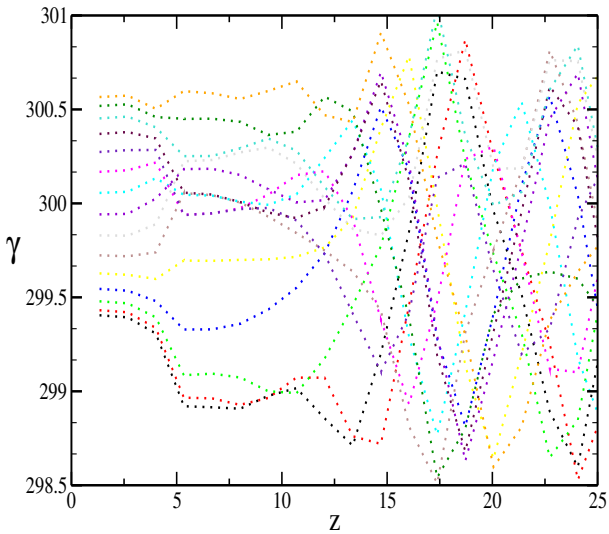

Figure 3: The variations of energy of the electrons as a function of the distance through the wiggler

(higher) efficiency. In the absence of tapering, oscillation of the radiation power beyond the saturation point persists. In one period, electrons give their energy to the radiation to increase the radiation amplitude and reduce the energy of electrons. This will cause the electrons to lose their resonance with the electromagnetic radiation and go to the phase in which they will extract energy from the radiation. Following this situation, the amplitude of radiation decreases up to the point at which electrons gain energy and their resonance with the radiation is established. This will cause the electrons to lose their energy to radiation. This cycle will repeat itself It has been shown that by decreasing the amplitude of

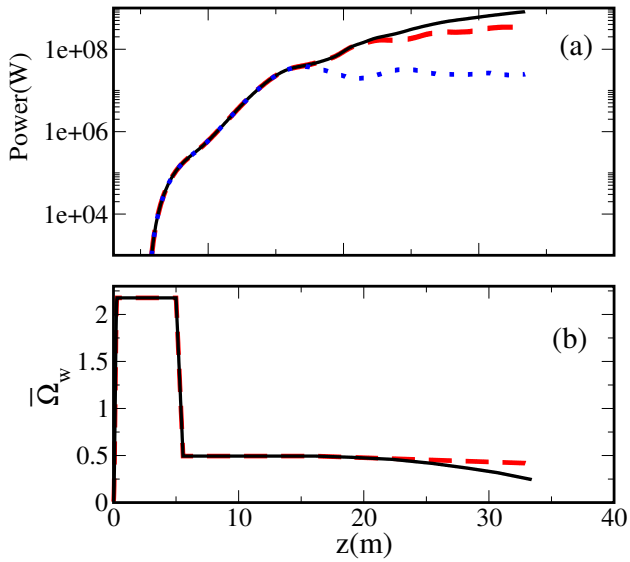

Figure 4: Comparison of the growth in the third harmonic power for a linearly tapered (dashed line), nonlinearly tapered (solid line), and untapered (dotted line) wiggler (a). Plot (b) shows Ω_w versus z for the linear tapering (dashed line) and nonlinear tapering (solid line) of the wiggler.

the wiggler a portion of the transverse energy of the electron beam will be transferred to the longitudinal motion and therefore accelerate the electron beam. This reduction can be linearly or linearly, that nonlinear decreasing can obtain more suitable restoration of the resonance condition.

It is assumed that the FEL has a constant wiggler field B_w (beyond the injection region) up to the point z_T (the saturation point), and after that the wiggler amplitude decreases linearly by the slope m. The linearly tapered wiggler may be written as

$$\overline{\Omega}_{wh}(\overline{z}) = \begin{cases} \overline{\Omega}_{wh}, & \overline{z} < \overline{z}_T \\ \overline{\Omega}_{wh} - m(\overline{z} - \overline{z}_T), & \overline{z} \geq \overline{z}_T \end{cases} \quad (7)$$

And the nonlinearly tapered wiggler can be as

$$\overline{\Omega}_{wh}(\overline{z}) = \begin{cases} \overline{\Omega}_{wh}, & \overline{z} < \overline{z}_{T1} \\ \overline{\Omega}_{wh} - m_i(\overline{z} - \overline{z}_{Ti}), & \overline{z}_{Ti} < \overline{z} < \overline{z}_{Ti+1} \end{cases} \quad (8)$$

$\overline{z}_{Ti+1}$ with $i = 1, 2, 3, \ldots$ are slopes of the lines between $\overline{z}_{Ti}$ and m_i. The second part of the wiggler in at apered harmonic lasing has been optimized over the entire length of 16.1 m. In Fig. 4(a), a comparison is made between the linearly tapered (dashed line), nonlinearly tapered (solid line), and untapered (dotted line) wigglers for the power of the third harmonic lasing. The wiggler amplitude is decreased at $z_T = 16.1\,m$ with the slope $m = 0.2\times10^{-4}$ for the linearly tapered wiggler. For nonlinear tapering, the amplitude of the wiggler is decreased at $z_{T1} = 16.1\,m$, $z_{T2} = 19\,m$, $z_{T3} = 22.6\,m$, $z_{T4} = 25.5\,m$, $z_{T5} = 28.3\,m$, $z_{T6} = 30.7\,m$ with slopes of $m_1 = 0.2\times10^{-4}$, $m_2 = 0.3\times10^{-4}$, $m_3 = 0.6\times10^{-4}$,

ISBN 978-3-95450-134-2

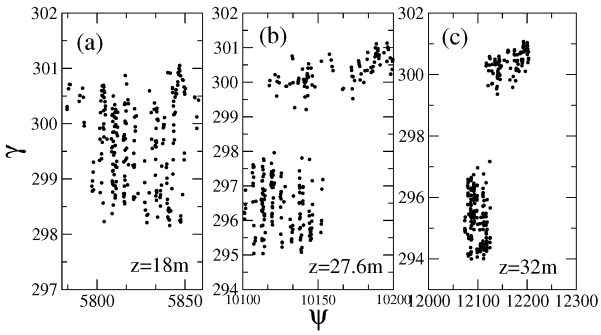

Figure 5: Distribution of energy γ versus the distribution of pondermotive phase of the electron beam at different values of the coordinate z along the linearly tapered wiggler.

$m_4 = 0.8\times10^{-4}$, $m_5 = 0.9\times10^{-4}$, $m_6 = 1.2\times10^{-4}$, respectively. The parameters m and z_T are chosen to obtain the maximum intensity of the third harmonic lasing, which are found by a successive run of the code. We can see significant increases in the third harmonic power from 3.8×10^7 to 8.1×10^8W for the linear tapering, and from to W for thenonlinear tapering. It can be seen that the nonlinear tapering of the wiggler amplitude with different slopes has higher efficiency. The profile for the variation of the wiggler parameter Ω_w with $z(m)$ for the nonlinear tapering (solid line) and linear tapering (dashed line) of the wiggler is shown in Fig. 4(b).

The longitudinal phase space of the electrons at different coordinates z along the linearly tapered wiggler is represented in Fig. 5. It can be seen that in the tapered region and beyond the energy of the electron beam is reduced. Because of the restoration of the resonance condition, electrons give their energy to the radiation and the radiation amplitude increases.

SAMMARY

In this paper, a one-dimensional simulation is conducted to analyze harmonic lasing FEL. In order to generate UV radiation, the fundamental resonance disrupted by reducing the undulator magnetic field and the third harmonic grows up to the saturation point. The thermal effect of the electron beam is taken into account. By relating the energy distribution function to the distribution function of the pondermotive phase,chaotic patterns at the saturation point are revealed. It is found that by suitably tapering the amplitude of the second wiggler field, saturation of the radiation for a shorter wavelength can be postponed leading to further amplification. In the case of the tapered wiggler, it is found that the efficiency can be enhanced more effectively by the nonlinear reduction of the second wiggler field at saturation point compared to that of the linear tapering.

REFERENCES

[1] W. Ackermann, G. Asova, V. Ayvazyan, A. Azima, N. Baboi, Nature Photon. 1, 336 (2007).

[2] R. Bonifacio, L. De Salvo, and P. Pierini, Nucl. Instrum.Methods Phys. Res., Sect. A 293, 627 (1990).

[3] H.P. Freund, S. Biedron, and S. Milton, Nucl. Instrum. Methods Phys. Res., Sect. A 445, 53 (2000).

[4] Z. Huang and K. Kim, Phys. Rev. E 62, 7295 (2000).

[5] E.L. Saldin, E. A. Schneidmiller, and M.V. Yurkov, Phys. Rev. ST Accel. Beams 9, 030702 (2006).

[6] D. Ratner, A. Brachmann, F.J. Decker, Y. Ding, D. Dowell, P. Emma, A. Fisher, J. Frisch, S. Gilevich, Z. Huang, P. Hering, et al., Phys. Rev. ST Accel. Beams 14, 060701 (2011).

[7] L.H. Yu, Phys. Rev. A 44, 5178 (1991).

[8] B.W.J. McNeil, G.R.M. Robb, M.W. Poole, and N.R. Thompson, Phys. Rev. Lett. 96, 084801 (2006).

[9] H.P. Freund and S.H. Gold, Phys,. Rev. Lett. 52, 926 (1984).

[10] P. Sprangle, C.M. Tang, and W.M. Manheimer, Phys. Rev. Lett.43, 1932 (1979).

[11] P. Sprangle, C.M. Tang, and W.M. Manheimer, Phys. Rev. A 21, 302 (1980).

[12] H.P. Freund and J. Pasour, Phys. Rev. Lett.91, 094801 (2003).

[13] X.J. Wang, T. Watanabe, Y. Shen, R.K. Li, J.B. Murphy, T. Tsang, and H.P, Freund, Appl. Phys. Lett.91, 181115 (2007).

[14] N.S. Mirian, M.H. Rouhani, `http://particles.ipm.ir/Cyrus1D.jsp`

[15] H.P. Freund, S.G. Biedron, and S.V. Milton, IEEE J. Quantum Electron.36, 275 (2000).

[16] H.P. Freund, L. Giannessi, and W.H. Miner, Jr, J. Appl. Phys. 104, 123114 (2008).

[17] H.P. Freund, S.G. Biedron, and S.V. Milton, IEEE J. Quantum Electron.27, 243 (2003).

[18] E. Salehi, B. Maraghechi, and N.S. Mirian, Phys. Plasmas 22, 033110 (2015).

ISBN 978-3-95450-134-2